

High-Resolution EXAFS of the Active Site of Human Sulfite Oxidase: Comparison with Density Functional Theory and X-ray Crystallographic Results

Hugh H. Harris,[†] Graham N. George,^{*,‡} and K. V. Rajagopalan[§]

School of Chemistry, University of Sydney, New South Wales 2006, Australia,
Department of Geological Sciences, University of Saskatchewan, Saskatoon,
Saskatchewan S7N 5E2, Canada, and Department of Biochemistry,
Duke University Medical Center, Durham, North Carolina 27710

Received July 22, 2005

Much of our knowledge about molybdenum enzymes has originated from EXAFS spectroscopy. This technique provides excellent bond-length accuracy but has only limited bond-length resolution. We have used EXAFS spectroscopy with an extended data range in an attempt to improve bond-length resolution for the molybdenum enzyme sulfite oxidase. The Mo site of sulfite oxidase has two oxygen and three Mo–S ligands (two from cofactor dithiolene plus a cysteine). For the oxidized (Mo^{VI}) enzyme, we find that the three Mo–S bond lengths are very similar (within 0.05 Å) at 2.41 Å, as are the Mo=O ligands at 1.72 Å. Density functional theory shows that this is consistent with the proposed active-site structure. The reduced (Mo^{IV}) enzyme shows two Mo–S bond lengths at 2.35 Å and one at 2.41 Å (assigned to cofactor dithiolene and cysteine, respectively, from DFT), together with one Mo=O at 1.72 Å and one Mo–OH₂ at 2.30 Å.

The mononuclear molybdenum enzymes all contain either one or two molybdopterin cofactors coordinated by a dithiolene motif to molybdenum, but their active sites show remarkable structural and functional diversity.¹ Currently, two techniques have provided quantitative structural information on molybdenum enzyme active sites: protein X-ray crystallography (PX) and X-ray absorption spectroscopy (XAS). Crystallography can provide a wealth of three-dimensional structural information but has only moderate accuracy for bond lengths. It has suffered from problems due to photoreduction of the metal site during data acquisition² and from multiple species cocrystallizing.³ XAS, on the other hand, is less prone to photoreduction and has

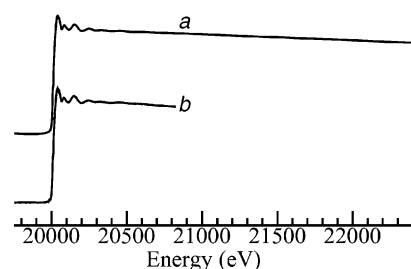


Figure 1. Comparison of oxidized sulfite oxidase raw data sets collected with (a) high resolution ($k_{\max} = 25.2 \text{ \AA}^{-1}$) and (b) normal ($k_{\max} = 14.5 \text{ \AA}^{-1}$) data ranges. Data acquisition times for a single scan were 55 and 35 min for plots a and b, respectively. The data shown in plot b is that of George et al.⁵

excellent accuracy in bond lengths but provides little or no three-dimensional information. Furthermore, XAS has only limited distance resolution (the ability to discriminate between similar bond lengths of similar atoms) when used with conventional data ranges. In this paper, we present a study of the active site of sulfite oxidase in which we attempt to overcome the limited resolution of XAS by significantly extending the data range. We have combined this with density functional theory (DFT) calculations to obtain additional three-dimensional structural insight into the active site.

Sulfite oxidase catalyzes the two-electron oxidation of sulfite to sulfate.⁴ This occurs at the molybdenum site, which is reduced from Mo^{VI} to Mo^{IV} in the process. The molybdenum is coordinated by the ene-1,2-dithiolate of the molybdopterin cofactor and a protein-based cysteine thiolate plus two oxo ligands in the Mo^{VI} form,⁵ one of which is converted to an –OH or –OH₂ in the Mo^{IV} form. As yet, the precise functional role of each of the ligands to the metal is not clear.

Figure 1 compares the raw Mo K-edge data from sulfite oxidase for a high-resolution XAS experiment with that of a conventional experiment. Extending the data to this extent

* To whom correspondence should be addressed. E-mail: g.george@usask.ca.

[†] University of Sydney.

[‡] University of Saskatchewan.

[§] Duke University Medical Center.

(1) Hille, R. *Trends Biochem. Sci.* **2002**, *27*, 360–367.

(2) George, G. N.; Pickering, I. J.; Kisker, C. *Inorg. Chem.* **1999**, *38*, 2539–2540.

(3) Li, H.-K.; Temple, C.; Rajagopalan, K. V.; Schindelin, H. *J. Am. Chem. Soc.* **2000**, *122*, 7673–7680.

(4) McLeod, R. M.; Farkas, W.; Fridovitch, I.; Handler, P. *J. Biol. Chem.* **1961**, *236*, 1841–1852. Cohen, H. L.; Betcher-Lange, S.; Kessler, D. L.; Rajagopalan, K. V. *J. Biol. Chem.* **1972**, *247*, 7759–7766.

(5) George, G. N.; Garrett, R. M.; Prince, R. C.; Rajagopalan, K. V. *J. Am. Chem. Soc.* **1996**, *118*, 8588–8592.

Table 1. Selected Geometric Parameters for Oxidized and Reduced Forms of the Sulfite Oxidase Active Site (See Figure 3)^a

	XAS (ox)	DFT (ox)	XAS (red.)	PX (red.) ¹⁰	DFT (red.) ^b	DFT (red.) ^c
Mo–S _{cys}	2.42	2.47	2.41	2.47	2.42	2.45
Mo–O _{api}	1.72	1.75	1.72	1.74	1.73	1.74
Mo–O _{eq}	1.72	1.75	2.30	2.25	2.34	2.08
Mo–S'	2.42	2.52	2.35	2.37	2.35	2.41
Mo–S''	2.42	2.50	2.35	2.38	2.40	2.46
S'–S''		3.20		3.19	3.19	3.24
S'–Mo–O _{eq}		131		139	134	137
S''–Mo–S _{cys}		154		147	138	151
O _{api} –Mo–S _{cys} –C _{cys}		46		82	108	98

^a Distances are in angstroms and angles in degrees. ^b Water is coordinated in place of the equatorial oxo ligand. ^c Hydroxide is coordinated in place of the equatorial oxo ligand.

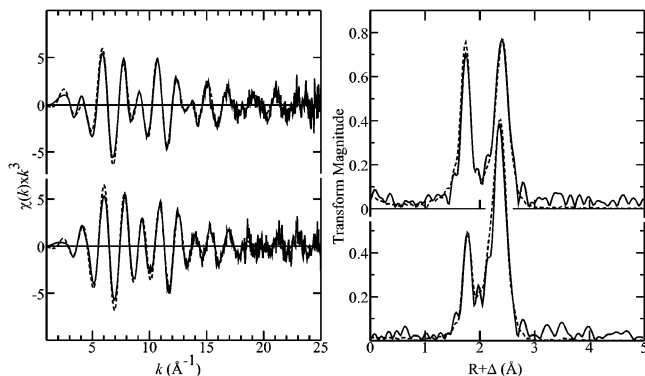


Figure 2. Molybdenum EXAFS of wild-type human sulfite oxidase in Mo^{VI} (top) and Mo^{IV} (bottom) forms. The solid lines show experimental data, while the broken lines show the best fit. EXAFS oscillations are shown to the left; corresponding Fourier transforms, shown at the right, are phase-corrected for Mo–O backscattering. The peaks at $R + \Delta \approx 1.7$ Å in the Fourier transforms arise from Mo=O EXAFS, while the peaks at $R + \Delta \approx 2.4$ Å arise from Mo–S, with a Mo–O component in the reduced form.

is experimentally challenging and requires excellent beamline stability; however, with modern beamline technology, we find that this is clearly achievable. Figure 2 shows the high-resolution EXAFS and Fourier transforms of oxidized and reduced enzyme^{6,7} together with the results of curve-fitting analyses, which are summarized in Table 1. The data and analyses are consistent with those of previous EXAFS work.^{2,5,8} The exact resolution of the data is a function of both the k range and the different EXAFS components present, but to a first approximation, it is given by $\pi/2k_{\max}$ or 0.06 Å for our data range. In the case of the Mo^{IV} form, discrete Mo–S distances at 2.35 and 2.41 Å are resolved (Table 1). This is not the case with the Mo^{VI} form, indicating that all three Mo–S bond lengths must be very close to the mean distance of 2.42 Å. In the unresolved Mo^{VI} case, the Debye–Waller factor (σ^2) can provide boundaries for Mo–S bond lengths.⁹ The observed σ^2 value for the Mo–S compo-

nent is consistent with a distribution of Mo–S bond distances such as 2.37, 2.42, and 2.47 Å or alternatively one at 2.37 Å and two at 2.45 Å.¹⁰ The Mo^{VI} form also has two short oxygen ligands at 1.72 Å, and the Mo^{IV} form, a single short oxygen ligand at 1.72 Å. The $R \sim 2.4$ Å region of the reduced data set includes both the expected Mo–S contributions and a long Mo–O bond at 2.30 Å, in good agreement with the PX analysis,¹¹ which suggested a Mo–O bond length of 2.25 Å for the photoreduced enzyme.^{12,13} The Mo–O interaction partially cancels with the single longer Mo–S component at 2.41 Å, facilitating the resolution of the Mo–S distances; significantly worse fits are generated by models with unresolved Mo–S distances or lacking the long Mo–O bond.

DFT energy minimizations^{14–16} using Becke exchange¹⁷ and Perdew correlation¹⁸ functionals (BP91), of the oxidized and reduced forms of the active site, agree well with the respective experimental data. The optimized geometries are shown in Figure 3, and selected geometrical parameters are given in Table 1. The well-known tendency of the BP91 nonlocal functional combination to overestimate bond distances (in this instance by as much as 0.1 Å) is evident in Table 1 and is likely exacerbated by the presence of the second-row element Mo.¹⁹

Allowing for this and comparing the Mo–O_{eq} distance from XAS and PX (~ 2.3 Å) with calculated values for hydroxide (2.08 Å) and water (2.34 Å) indicate that a water ligand is responsible for the equatorial oxygen coordination to the reduced Mo center.²⁰ The lowest-energy structures for

(6) Garrett, R. M.; Rajagopalan, K. V. *J. Biol. Chem.* **1996**, *271*, 7387–7391.

(7) Human recombinant sulfite oxidase was prepared as previously described.⁶ The oxidized sample was prepared at a final concentration of approximately 1.7 mM in a mixed buffer system consisting of 20 mM Tris, bis-Tris, and bis-Tris propane (pH 9.0) with no added chloride and was frozen in a 10 mm × 10 mm × 3 mm leucite cell. The reduced sample was generated from the oxidized sample by the addition of excess dithionite and trace methylviologen.

(8) George, G. N.; Kipke, C. A.; Prince, R. C.; Sunde, R. A.; Enemark, J. H.; Cramer, S. P. *Biochemistry* **1989**, *28*, 5075–5080.

(9) The value for σ^2 is made up of the sum of static (differing bond distances) and vibrational components ($\sigma^2 = \sigma_{\text{stat}}^2 + \sigma_{\text{vib}}^2$). σ^2 for the Mo–S component from the best fit is ca. 0.0039 Å², while for the Mo–O component, $\sigma^2 \sim 0.0022$ Å². Because the Mo=O bonds are likely stronger than Mo–S (σ^2 for M=O < σ^2 for M–S) and DFT suggests the two Mo=O distances are equal (giving $\sigma_{\text{stat}}^2 = 0$), a rough estimate of the high boundary for the static contribution to σ^2 for the Mo–S component is the difference between the overall σ^2 for both components, giving 0.0017 Å². σ_{vib}^2 for Mo–S can also be calculated using the methods described by Poiarkova and Rehr, giving a value of 0.0023 Å² (force constant for Mo–S of 135 N/m derived from IR spectroscopy; bond length of 2.41 Å; Poirakova, A. V.; Rehr, J. J. *J. Synchrotron Radiat.* **1999**, *6*, 313–314), and σ_{stat}^2 is thus 0.0020 Å², a three-way split with a bond-length distribution of 0.055 Å.

(10) We note that these are arbitrarily chosen examples and that there are many possible solutions.

(11) Kisker, C.; Schindelin, H.; Pacheco, A.; Wehbi, W. A.; Garrett, R. M.; Rajagopalan, K. V.; Enemark, J. H.; Rees, D. C. *Cell* **1997**, *91*, 973–983.

(12) The enzyme used in the XRD study was initially oxidized, but the structure has been assigned to a reduced form because photoreduction of the crystallographic sample is likely as a result of a number of factors.

(13) X-ray absorption near-edge spectra are highly sensitive to the electronic structure. We observed no changes in the near-edge spectrum throughout the course of our experiment, indicating that no significant photoreduction occurred.

(14) DMol³ Materials Studio, version 2.1.

(15) Delley, B. *J. Chem. Phys.* **1990**, *92*, 508–517. Delley, B. *J. Chem. Phys.* **2000**, *113*, 7756–7764.

(16) Nonlocal corrections were applied during the evaluation of both potential and energy. Double numerical basis sets included polarization functions for all atoms. Calculations were spin-unrestricted, and effective core potentials were used in place of Mo core orbitals ($n = 1–3$). No symmetry constraints were applied. Optimization energy tolerances of 1.0×10^{-5} Hartree were used, but no vibrational analyses were performed.

(17) Becke, A. D. *J. Chem. Phys.* **1988**, *88*, 2547–2553.

(18) Perdew, J. P.; Wang, Y. *Phys. Rev. B* **1992**, *45*, 13244–13249.

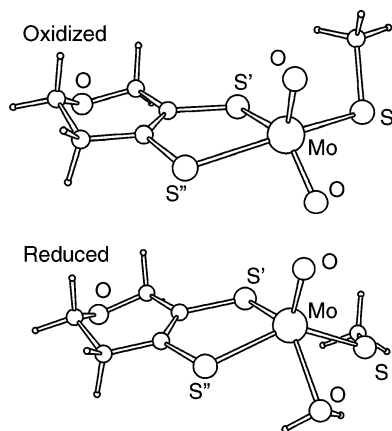


Figure 3. DFT geometry-optimized structures of the oxidized and reduced forms of the active site of sulfite oxidase with a truncated pyranopterin cofactor. Methane thiolate is substituted for cysteine. The considered theoretical models for the reduced form have either hydroxide or water in place of the equatorial oxo group. In the figure, unlabeled atoms are either carbon or hydrogen (small spheres).

both hydroxide- and water-coordinated reduced sulfite oxidase have short H–S_{cys} bond distances (2.43 and 2.20 Å, respectively), indicating significant hydrogen-bonding interactions. A second local energy minimum (ca. 1 kcal/mol higher in energy than the global minimum) was found for the water-coordinated structure that also includes a second hydrogen bond from water to the O_{api} atom at 2.85 Å. This geometry seems unfavorable, however, because the apical oxo group is in a far more heavily crowded environment in the reported crystal structure than that of the cysteinyl sulfur.

The geometry at the molybdenum in both oxidized (DFT) and reduced (DFT and PX) forms is significantly distorted from square pyramidal, most notably in the S'–Mo–O_{eq} angle. The EXAFS data indirectly support this for both forms because no oxo trans effect on the S'–Mo distance is observed. A geometry optimization on the Mo^{VI} form (see Figure 2) with the S'–Mo–O_{api} angle constrained to linear provides a S'–Mo distance of 2.67 Å, which would be easily resolved in our EXAFS data.

The largest deviation of the DFT results from the PX analysis is in the O_{api}–Mo–S_{cys}–C_{cys} torsion angle. Crystallography gives a value of 82°, while DFT gives values of 46° for the Mo^{VI} form and 108° for the lowest-energy water-coordinated Mo^{IV} form. This discrepancy can be attributed to the effects of the protein environment that are not incorporated in the calculations in which the cysteinyl C atom is essentially untethered. It is interesting that the direction of torsional distortion away from the PX structure is reversed for the different oxidation states. We calculate that the energy relaxation away from the constrained angle of 82° is quite low, less than 2 kcal/mol for both the oxidized and reduced forms. We also calculate that variation in this torsional angle affects the strength of the bound water to cysteinyl sulfur hydrogen bond in the reduced form and hence the ease of the enzymatically necessary breaking of the water O–H bond. This can be observed in the reduced form with the

torsion angles constrained at 46, 82, and 108°, where the calculated H–S_{cys} bond distances are 2.21, 2.35, and 2.20 Å, respectively.

Rotation around the Mo–S dihedral angle will clearly be restrained to some extent by the surrounding protein, and it is not clear which of these angles are relevant in the protein environment; hybrid quantum mechanical/molecular mechanical calculations may provide further insight into this issue. Not only has this torsion angle been implicated in modulating the redox potential of the Mo center,²¹ but on the basis of the observed hydrogen bonding in our calculations, it may be important in lowering the activation barrier for the dissociation of water and controlling the egress of protons during the regeneration stage of the enzymatic cycle.

In conclusion, our combined EXAFS and DFT results indicate that the equatorial O-donor ligand in the reduced form of human sulfite oxidase is most likely a water and not a hydroxide. This is consistent with electrochemical results for the human enzyme²² but not those reported for a bacterial sulfite dehydrogenase.²³ We are also able to resolve the Mo–S_{cys} bond length from the dithiolene Mo–S bonds in the reduced form of the enzyme.

Acknowledgment. Portions of this work were carried out at the Stanford Synchrotron Radiation Laboratory, which is funded by the U.S. Department of Energy, Office of Basic Energy Sciences and Office of Biological and Environmental Sciences, and the National Institutes of Health, National Center for Research Resources. H.H.H. acknowledges support from an Australian Synchrotron Research Program Postdoctoral fellowship and an Australian Research Council Discovery Program grant (Grant DP346162). Research at the University of Saskatchewan (G.N.G.) was supported in part by Canada Research Chair award, the University of Saskatchewan, the Province of Saskatchewan, the National Institutes of Health (Grant GM5735), the Natural Sciences and Engineering Research Council (Canada; Grant 283315), and the Canadian Institute of Health Research. Work at Duke University was supported by the National Institutes of Health (Grant GM44283).

Supporting Information Available: Tables of EXAFS curve-fitting parameters and Cartesian coordinates for DFT-minimized structures, figures of HOMO + LUMO isosurfaces for oxidized and reduced active sites, and detailed experimental information. This material is available free of charge via the Internet at <http://pubs.acs.org>.

IC0512274

- (19) Scheiner, A. C.; Baker, J.; Andzelm, J. W. *J. Comput. Chem.* **1997**, *18*, 775–795.
- (20) It is assumed here that X-ray photoreduction completely reduced the Mo site on the protein crystallography to Mo^{VI} and calculations were performed with the appropriate overall charge of 1– for water-bound structures and 2– for hydroxide-bound structures.
- (21) McNaughton, R. L.; Tipton, A. A.; Rubie, N. D.; Conry, R. R.; Kirk, M. L. *Inorg. Chem.* **2000**, *39*, 5697–5706.
- (22) Hille, R. *Chem. Rev.* **1996**, *96*, 2757–2816.
- (23) Aguey-Zinsou, K.-F.; Bernhardt, P. V.; Kappler, U.; McEwan, A. G. *J. Am. Chem. Soc.* **2003**, *125*, 530–535.